MOLECULAR
METABOLISM

Glucagon-like peptide-2 pharmacotherapy activates hepatic Farnesoid X receptor-signaling to attenuate resection-associated bile acid loss in mice

Johannes Reiner[1,*], Nooshin Mohebali[1], Jens Kurth[2], Maria Witte[3], Cornelia Prehn[4], Tobias Lindner[5], Peggy Berlin[1], Nagi Elleisy[1], Robert H. Förster[1], Alexander Cecil[4], Robert Jaster[1], Jerzy Adamski[4], Sarah M. Schwarzenböck[2], Brigitte Vollmar[6], Bernd J. Krause[2], Georg Lamprecht[1]

ABSTRACT

Objective: Villus growth in the small bowel by Glucagon-like peptide-2 (GLP-2) pharmacotherapy improves intestinal absorption capacity and is now used clinically for the treatment of short bowel syndrome and intestinal failure occurring after extensive intestinal resection. Another recently acknowledged effect of GLP-2 treatment is the inhibition of gallbladder motility and increased gallbladder refilling. However, the impact of these two GLP-2-characteristic effects on bile acid metabolism in health and after intestinal resection is not understood.

Methods: Mice were injected with the GLP-2-analogue teduglutide or vehicle. We combined the selenium-75-homocholic acid taurine (SeHCAT) assay with novel spatial imaging in healthy mice and after ileocecal resection (ICR mice) and associated the results with clinical stage targeted bile acid metabolomics as well as gene expression analyses.

Results: ICR mice had virtual complete intestinal loss of secondary bile acids, and an increased ratio of 12α-hydroxylated vs. non-12α-hydroxylated bile acids, which was attenuated by teduglutide. Teduglutide promoted SeHCAT retention in healthy and in ICR mice. Acute concentration of the SeHCAT-signal into the hepatobiliary system was observed. Teduglutide induced significant repression of hepatic cyp8b1 expression, likely by induction of MAF BZIP Transcription Factor G.

Conclusions: The data suggest that GLP-2-pharmacotherapy in mice significantly slows bile acid circulation primarily via *hepatic* Farnesoid X receptor-signaling.

1. INTRODUCTION

Enterohormones orchestrate the digestive process by modulating gastrointestinal secretions and motility, epithelial function and visceral blood flow. Glucagon-like peptide-2 (GLP-2) is an enterohormone secreted from L-cells in the distal gastrointestinal tract upon ingestion of nutrients [1]. GLP-2 is a 33 amino acid peptide hormone cleaved from Proglucagon, which is encoded by the Pre-proglucagon gene [2]. The most striking effect of exogenous GLP-2-stimulation, villus growth in the small bowel, was discovered ~25 years ago [3] and improves intestinal absorption capacity in mice and humans [4,5]. This effect is now used clinically for the treatment of intestinal failure, which typically occurs after major intestinal resection involving the ileum as the main site of bile acid reabsorption

[6,7]. The second and more recently observed striking effect of exogenous GLP-2-stimulation is inhibition of gallbladder motility and increased gallbladder refilling [8,9]. This effect has been suggested to contribute to an increased risk of cholelithiasis [9].

However, the impact of these two GLP-2-characteristic effects on bile acid metabolism after intestinal resection is not understood.

Bile acid metabolism is a complex and tightly regulated system, involving de novo synthesis from cholesterol, conjugation for solubilization, secretion and storage in the biliary system, as well as intestinal reabsorption, and back flow to the liver via the portal vein in the enterohepatic circulation (EHC). Importantly, besides the function of bile salts as detergents in the intestinal lumen, bile acids bind to the farsenoid X receptor (FXR), primarily to regulate their own metabolism [10]. Of note, the system shares most important features in mice and

[1]Division of Gastroenterology and Endocrinology, Department of Medicine II, Rostock University Medical Center, Rostock, Germany [2]Department of Nuclear Medicine, Rostock University Medical Center, Rostock, Germany [3]Department of General, Visceral, Thoracic, Vascular and Transplant Surgery, Rostock University Medical Center, 18057 Rostock, Germany [4]Metabolomics and Proteomics Core (MPC), Helmholtz Zentrum München, Germany [5]Core Facility Multimodal Small Animal Imaging, Rostock University Medical Center, Rostock, Germany [6]Rudolf-Zenker-Institute for Experimental Surgery, Rostock University Medical Center, 18057 Rostock, Germany

*Corresponding author. Division of Gastroenterology and Endocrinology, Department of Medicine II, Rostock University Medical Center, Germany. E-mail: Johannes.reiner@med.uni-rostock.de (J. Reiner).

humans, including the presence of a gallbladder (which is not present in rats). Two important differences are the predominance of hydroxylated muricholic acid in mouse bile and the preference for taurine-instead of glycine-conjugation.

Exogenous GLP-2 may interfere with bile acid metabolsm via two different mechanisms. 1) it may increase bile acid reabsorption by inducing small intestinal growth. Through the *intestinal* Fxr-feedback loop involving Fgf-15, the mouse homolog of human FGF-19, this would reduce de novo synthesis by repressing Cyp7a1, which mediates the rate limiting step in hepatic cholic acid synthesis. 2) by slowing enterohepatic circulation through retention of bile acids in the hepatobiliary system (HBS). The latter would stimulate *hepatic* Fxr signaling to inhibit de novo synthesis of primary unconjugated bile acids. *Hepatic* Fxr represses Cyp8b1 to reduce 12-alpha-conjugation capacity, but this is not a rate limiting step under steady state [11].

To estimate pharmacologic effects of GLP-2 therapy on bile acid circulation and metabolism after ileocecal resection (ICR) in mice, we used a spatially resolved selenium-75-homocholic acid taurine (SeHCAT) test, gene expression analyses and targeted metabolomics. Here, we show that GLP-2-pharmacotherapy in mice slows bile acid circulation by affecting both the biliary as well as the enteral limb of the EHC to converge on *hepatic* Fxr signalling.

2. RESEARCH DESIGN AND METHODS

2.1. Mice

All animal experiments were performed according to European Union Directive 2010/63/EU and were approved by the local animal welfare authority (Landesamt für Landwirtschaft, Lebensmittelsicherheit und Fischerei Mecklenburg-Vorpommern, 7221.3-1.1-008/16 and 7221.3-1.1-021/20). C57BL6/J mice were purchased from The Jackson Laboratory (Bar Harbor, ME) and bred in the animal facilities at the Rudolf-Zenker-Institute for Experimental Surgery, University Medical Center Rostock. Mice were housed in groups of up to five at a 12 h light−dark cycle (dark: 7 pm−7 am), a temperature of $21 \pm 2\ ^{\circ}C$ and relative humidity of $60 \pm 20\%$ with free access to standard chow (pellets, 10 mm, ssniff-Spezialdiäten GmbH, Soest, Germany) until the start of the experiment with free access to standard chow and water until surgical intervention. A timeline of the experiments is shown in Figure 1A. Adult male mice (body weight ∼30 g) at the mean age of 3−6 months were randomly assigned to one of the following groups: non-ICR mice received injections twice daily at 8 am $\pm$ 30 min and 8 pm $\pm$ 30 min, respectively, from day 1 to day 9, as (a) vehicle (volume-adjusted PBS) and (b) teduglutide (0.1 mg/kg BW). Alongside, ICR mice were operated on day 0, then received injections twice daily at 8
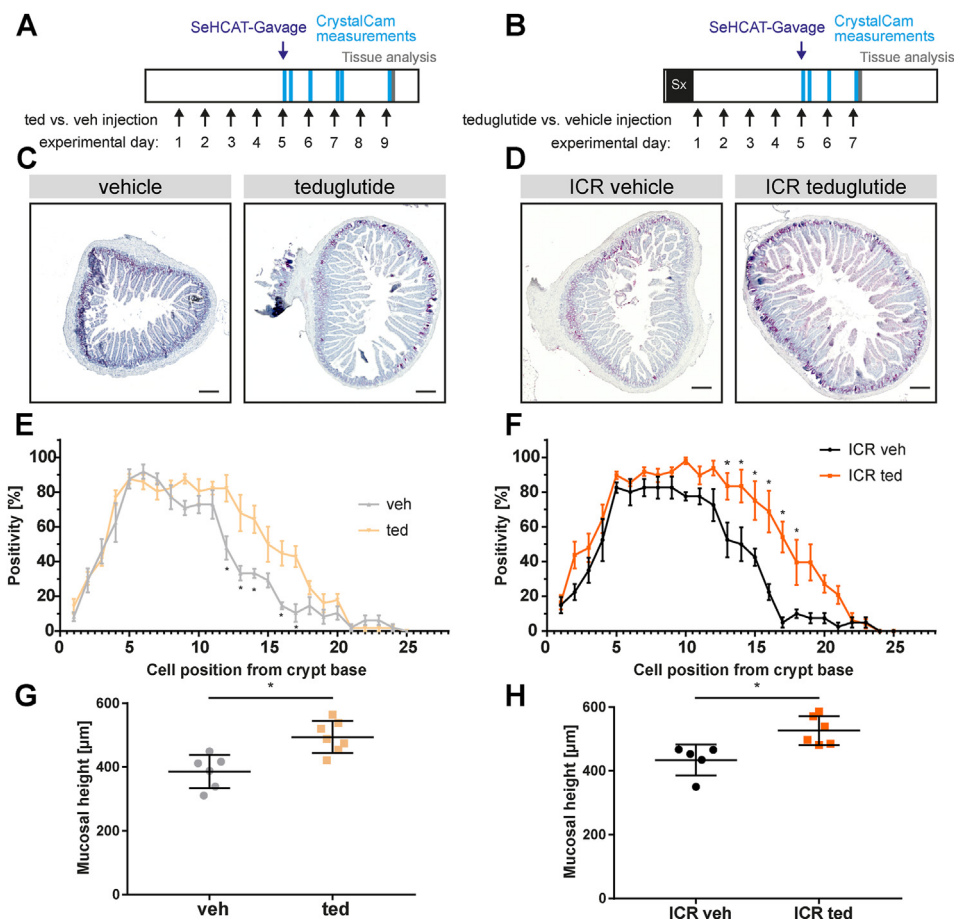
Figure 1: GLP-2 pharmacotherapy promotes mucosal growth. (A) Design for main experiment 1 with non-ICR mice. (B) Design for main experiment 2 with ICR mice. At the end of the experiments blood, intestine and liver tissue was collected and analyzed. (C) Representative images of proximal jejunum from non-ICR mice stained for ki-67. (D) Representative images of proximal jejunum from ICR mice stained for ki-67. (E) positivity for ki-67 was counted along the crypt base in non-ICR, vehicle (veh) and teduglutide (ted)-injected mice, n = 6 and 7, mean $\pm$ SEM. *p < 0.05, one-way ANOVA. (F) positivity for ki-67 was counted along the crypt base in ICR veh and ted mice, n = 5 and 6, mean $\pm$ SEM. *p < 0.05, one-way ANOVA. (G) Mucosal height was measured in non-ICR mice, n = 6 and 7, mean $\pm$ SD, *p < 0.05, unpaired t-test. (H) Mucosal height was measured in non-ICR mice, n = 5 and 6, mean $\pm$ SD, *p < 0.05, unpaired t-test.

 www.molecularmetabolism.com

am $\pm$ 30 min and 8 pm $\pm$ 30 min, respectively, from day 1 to day 7, as (c) vehicle (volume-adjusted PBS) and (d) teduglutide (0.1 mg/kg BW). For SeHCAT and gene expression analyses, group (a) was compared to group (b), whereas group (c) was compared to group (d) For bile acid pool analyses, two separate groups were included as controls. For the non-ICR arm, a group (e) was included, receiving vehicle injections twice daily at 8 am $\pm$ 30 min and 8 pm $\pm$ 30 min, from day 1 to day 9, but fasted for 12 h before autopsy. For the surgical arm, a sham operated group (f) was included, as a plausibility control - operated on day 0, then received vehicle injections twice daily at 8 am $\pm$ 30 min and 8 pm $\pm$ 30 min, respectively, from day 1 to day 7. Group allocation was done randomized, according to a prespecified order list, in order to minimize confounding from surgical day. Injections were done blockwise, alternating treatment and vehicle group. ICR and non-ICR groups were done in parallel. Injections were not blinded. Teduglutide (Revestive®) was purchased through the hospital pharmacy.

2.2. Ileocecal resection surgery procedures

For surgery, mice were weighed and anesthetized by intraperitoneal injection of ketamine (100 mg/kg bw) and xylazine (15 mg/kg bw). The operative technique of ileocecal resection was performed as described previously [12]. In brief, the ileocecal junction and the ileum were eviscerated through a midline incision. In mice undergoing ileocecal resection (ICR), the mesenteric blood vessels of the resected segment were ligated using clips (Weck, Horizon; Teleflex Medical, Kernen, Germany), and the intestine was divided 11 cm proximal to the ileocecal junction and immediately distal to the cecum. Ileum and cecum were resected, and an end-to-end, full-thickness jejunocolic anastomosis with interrupted stiches using a 10-0 monofilament suture (Ethilon; Ethicon, Norderstedt, Germany) was created under an operating microscope. Sham control mice received a single transection and reanastomosis 11 cm proximal to the cecum without resection. Immediately after extubation, all mice were weighted and resuscitated with subcutaenous injection of 1 ml saline and 5 mg/kg carprofen as an analgesic. Mice were allowed to recover in a heated terrarium (29 °C) for $\sim$ 4 h and then returned to cages with free access to liquid food and water.

2.3. Animal interventions

All mice were placed in single cages, in order to allow determination of individual food intake, stool consistency, and to prevent co-coprophagy in the SeHCAT-experiments. To prevent intestinal obstruction in the resected mice, these mice were switched to liquid diet (AIN 93G; Ssniff, Soest, Germany) 2 days before operation. For comparability of groups, all mice received this liquid diet from two days before the start of the experiment until the end of the observation period. Body weight and food intake were measured daily. Stool water content was analyzed on days 0, 2 and 7 of the experiment. EDTA-blood was drawn by retroorbital puncture on the final day of the experiment. Plasma was obtained after centrifuging at 4,000 U/min for 15 min. Plasma was frozen at -20 °C and shipped on dry ice from Rostock to Munich for bile acid metabolome analysis.

2.4. SeHCAT retention-test

SeHCAT retention test was performed with cohorts of mice which were pretreated as shown in Figure 1A. The SeHCAT capsule (GE Healthcare) of 370 kBq was dissolved and activity of approximately 20.5 Mbq was orally gavaged. Then, mice were anesthetized with inhaled isoflurane and placed with the abdomen in the center of the 4×4 cm^2 field of view of the portable CrystalCam (Crystal Photonics, Berlin, Germany) (Figure 2). To improve sensitivity, the camera has

been used uncollimated as also recommend for clinical applications [13]. Spatial imaging was performed for 120 s using an energy window of 40$-$400 keV in order to include the high- and the low energy peak of ^{75}Se. The measurements were performed at the following times: for non-ICR mice immediately (0 h), 4 h, 24 h, 48 h, and 96 h after gavage; for non-ICR mice immediately (0 h), 4 h, 24 h, 48 h after gavage. Of note, for the acute study, the measurement was performed right before injection of teduglutide 0.1 mg/kg BW, and 1 h after injection. Focus ratio was calculated from the highest signal intensity in the center compared to the lower signal intensity background around. At the final day of the experiment, mice were pseudonymized, to allow blinding of outcome measures. After the final whole-body image was taken, and cervical dislocation, the intestine was completely removed, then measured on the CrystalCam. The hepatobiliary system, including liver and the intact gall bladder, was removed and imaged in the same manner. Intestine/HBS-ratio was calculated from the signal intensities. In vehicle-injected ICR mice, the signal from the intestine was below the lower limit of detection in 2/5 mice in teduglutide treated mice, the signal from the intestine was below the lower limit of detection in 2/6 mice. These data points were excluded from the statistical analysis. Observation period of 96 h for non-ICR mice was chosen pragmatically: it has previously been shown that 24 h-fecal SeHCAT-excretion rate is 20$-$50% in rodents with intact EHC [14]. The observation period of 48 h for ICR-mice was chosen pragmatically: it has previously been shown that SeHCAT-retention after ileal resection in man is reduced to only $\sim$10% of non-ICR man within less than 72 h. The ideal point of time to measure differences attributable to ileal resection was deemed the half total observation period in man [15].

2.5. Plasma bile acid metabolome analysis

Mouse plasma bile acids were analyzed using LC-ESI-MS/MS technology and the AbsoluteIDQTM Bile Acids kit (Biocrates Life Sciences AG, Innsbruck, Austria), see Table 1. Compound identification and quantification were based on scheduled multiple reaction monitoring measurements (sMRM). The complete assay procedures of the Bile Acids kit and the results of an inter-laboratory ring trial have been described in detail previously [16,17].

In short: the extracts were diluted with 60 μL ultrapure water, cooled at 10 °C for LC-MS/MS measurements. The LC-separation was performed using 10 mM ammonium acetate in a mixture of ultrapure water/formic acid v/v 99.85/0.15 as mobile phase A and 10 mM ammonium acetate in a mixture of methanol/acetonitrile/ultrapure water/formic acid v/v/v/v 30/65/4.85/0.15 as mobile phase B. Bile acids were separated on the UHPLC column for BiocratesTM Bile Acids Kit (Product No. 91220052120868) combined with the precolumn SecurityGuard ULTRA Cartridge C18/XB-C18 (for 2.1 mm ID column, Phenomenex Cat. No. AJ0-8782). All solvents that have been used for sample preparation and measurement were of HPLC grade. Mass spectrometric analyses were done on an API 4000 triple quadrupole system (SCIEX Deutschland GmbH, Darmstadt, Germany) equipped with a 1260 Series HPLC (Agilent Technologies Deutschland GmbH, Böblingen, Germany) and a HTC-xc PAL auto sampler (CTC Analytics, Zwingen, Switzerland) controlled by the software Analyst 1.6.2. Data evaluation for quantification of metabolite concentrations and quality assessment were performed with the software MultiQuant 3.0.1 (Sciex) and the MetIDQ™ software package. Metabolite concentrations were calculated using internal standards and reported in μM. The ratios for taurine-over unconjugated as well as for 12α-hydroxylated vs non-12α-hydroxylated primary bile acids was calculated.
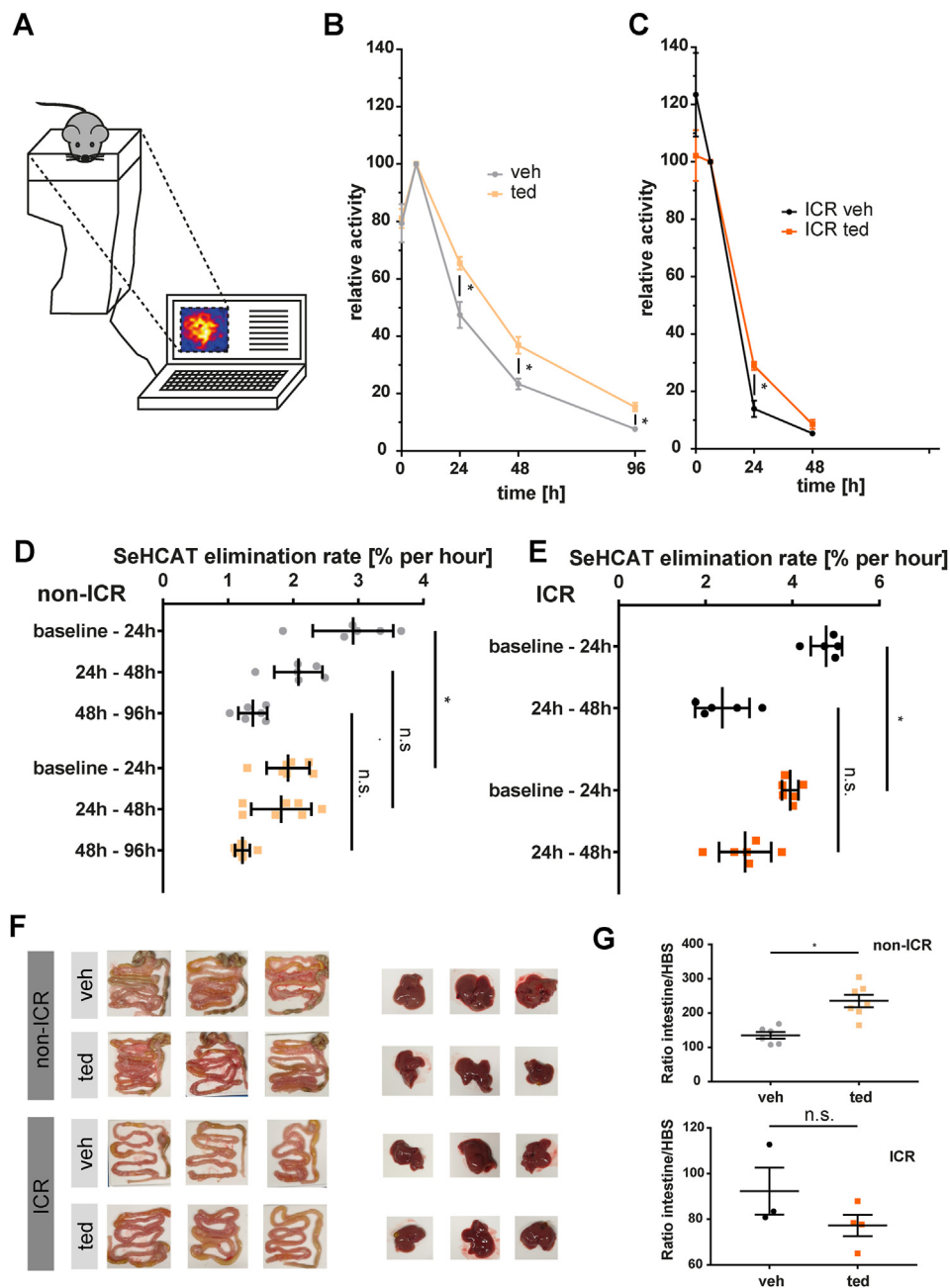
Figure 2: GLP-2 pharmacotherapy slows enterohepatic recirculation. (A) Setup for determination of SeHCAT retention. (B) Time course of relative whole body activitiy for non-ICR mice, injected with teduglutide (ted) or vehicle (veh), normalized to baseline at t = 6 h, n = 6 and 7 per group, mean ± SEM, *p < 0.05, multiple t-tests, corrected by FDR (Benjamini, Krieger, and Yekutieli) (C) time course of relative whole body activitiy for ICR mice, normalized to baseline at t = 6 h, n = 5 and 6 per group, mean ± SEM, *p < 0.05, multiple t-tests, corrected by FDR (Benjamini, Krieger, and Yekutieli) (D) SeHCAT elimination rate in non-ICR mice, n = 6,7, mean ± SD, *p < 0.05, one-way ANOVA. (E) SeHCAT elimination rate in non-ICR mice, n = 6,7, mean ± SD, *p < 0.05, one-way ANOVA. (F) Representative images from CrystalCam-scans of intestine and liver on the final day of the experiment ex vivo. (G) Of intestinal signal vs. hepatobiliary signal ex vivo, n = 6,7,3,4 (veh, ted, ICR veh, ICR ted), mean ± SEM, *p < 0.05, paired t-test.

2.6. RNA expression

Immediately after the final in vivo measurement, the ileum segment 13 cm proximal of the ileocecal junction in non-ICR mice and 2 cm proximal of the ileocolonic anastomosis in ICR mice was obtained and placed for histology. RNA was isolated with the RNeasy Mini Kit (Qiagen, Hilden, Germany) according to the manufacturers' instructions. Frozen tissue (~30 mg) was placed in lysis buffer and then mechanically disrupted with a bead beater (TissueLyser LT;

Qiagen, Hilden, Germany) at 50 Hz for 5 min with 7-mm stainless-steel beads (Qiagen, Hilden, Germany). The process included 15 min DNA digestion at room temperature using the RNase-free DNase set (Qiagen). For cDNA synthesis, 2 μg RNA was transcribed using the High-Capacity cDNA Reverse Transcription Kit (Thermo Fisher Scientific, Schwerte, Germany) according to the manufacturer's instructions. Taqman-probes were *Nr0b2* (Mm00 442278_m1), *Nr1h4* (Mm00436425_m1), *Actb* (Mm00607939_s1),

Table 1 — List of metabolites measured with the Biocrates® Bile Acids Kit MPC Metabolomics Platform, Helmholtz Zentrum München.	
Bile Acids (20)	
CA	Cholic acid
CDCA	Chenodeoxycholic acid
DCA	Deoxycholic acid
GCA	Glycocholic acid
GCDCA	Glycochenodeoxycholic acid
GDCA	Glycodeoxycholic acid
GLCA	Glycolithocholic acid
GUDCA	Glycoursodeoxycholic acid
HDCA	Hyodeoxycholic acid
LCA	Lithocholic acid
MCA(a)	Alpha-muricholic acid
MCA(b)	Beta-muricholic acid
MCA(o)	Omega-Murichoclic acid
TCA	Taurocholic acid
TCDCA	Taurochenodeoxycholic acid
TDCA	Taurodeoxycholic acid
TLCA	Taurolithocholic acid
TMCA (a+b)	Tauromuricholic acid (sum of alpha and beta)
TUDCA	Tauroursodeoxycholic acid
UDCA	Ursodeoxycholic acid

Cyp7a1 (Mm00484150_m1), *Cyp8b1* (Mm00501637_s1), *Cyp27a1* (Mm00470430_m1), *Fgfr4* (Mm01341852_m1), *Hnf4a* (Mm0 1247712_m1), *Mafg* (Mm00521961_g1), *Vil1* (Mm00494146_m1), *Fgf15* (Mm00433278_m1), *Slc10a2* (Mm00488258_m1). ΔCt was calculated in the ileum against the epithelium-specific marker *Vil1*, and in the liver against *Actb*.

2.7. Histology

Immediately after the final in vivo measurement, the ileum segment 12 cm proximal of the ileocecal junction in non-ICR mice and 1 cm proximal of the ileocolonic anastomosis in ICR mice was obtained and placed for histology in 4% paraformaldehyde. After 24 h, tissue was dehydrated, paraffin-embedded and stored at RT. For quantification of villus height, 5 μm thick tissue slides were made, hematoxylin and eosin-stained and five well-oriented, full-length crypts and villi per sample were measured and averaged using an Axio Observer inverted microscope (Zeiss) and Zen 2.3 software. To evaluate proliferative activity, ki-67 was immunohistochemically stained using ImmPress polymer reaction (Vector Laboratories) with the Ki-67 Monoclonal Antibody SolA15, eBioscience™, catalogue-no.: 14-5698-80. For quantification of proliferative activity, each cell position from the crypt base to cell position 25 was manually scored for presence or absence of ki-67-positivity.

2.8. Statistical analysis

Sample size calculation was done for the following three primary outcomes: a) SeHCAT retention at the final day of the experiment, b) overall plasma bile acid concentration, c) expression change in cyp7a1, for β = 0.2, using SPSS. The data were analyzed using GraphPad Prism 7.05 (GraphPad Software). Data are presented as means ± SD/SE or median for the indicated number of mice (n) per group. Data from mice with any preanastomotic bowel distension (deemed due to stenosis) was not included in the statistical analysis. In the case of normal distribution, and groupwise comparison, student's t test was applied. In the case of nonparametric distribution, Mann—Whitney U-test was applied. Multiple group comparisons were performed by One-way ANOVA or the nonparametric Kruskal—Wallis test correcting with the Dunn's test for multiple testing, as indicated. p values of <0.05 were considered significant.

3. RESULTS

3.1. Pharmacologic GLP-2-stimulation promotes bile acid retention via enhanced intestinal uptake

In order to recapitulate the known actions of GLP-2-pharmacotherapy, villus length and ki-67-index were measured in the jejunum. As expected, treatment with teduglutide enhanced proliferation, as indicated by the amount of ki-67-positive cells in the small intestine crypts in both non-ICR as well as ICR mice (Figure 1C—F). This expansion of proliferating cells was accompanied by strong villus growth at day 7 in the teduglutide treated groups (Figure 1G,H). Next, the effect of teduglutide on enterohepatic bile acid circulation was characterized (Figure 2A). First, SeHCAT retention was determined in non-ICR mice, which were treated with teduglutide and compared to vehicle-injected non-ICR mice. In vehicle-injected non-ICR mice, SeHCAT retention decreased over time from 100% to 47% after 24 h, 23% after 48 h and 7% after 96 h. Teduglutide-injected non-ICR mice had significantly increased SeHCAT retention, with 65% after 24 h, 39% after 48 h, and 14% after 96 h (Figure 2B). In vehicle-injected non-ICR mice, the elimination rate of SeHCAT was highest in the first 24 h (Figure 2D), but not significantly different between the different time intervals. In vehicle-injected ICR mice, SeHCAT retention was only 14% after 24 h and 5% after 48 h, well corresponding to the intestinal loss of primary bile acids (Figure 2C). In teduglutide-injected ICR mice SeHCAT retention was significantly increased to 29% after 24 h and it was 10% after 48 h (Figure 2C). Of note, SeHCAT elimination rate was significantly slowed by teduglutide compared to the vehicle-injected ICR mice in the first 24 h (Figure 2E). Because in the first 24 h after gavage of SeHCAT, intestinal uptake is the major determinant of incorporation into the EHC [18], the SeHCAT-signal in the intestine vs. the HBS was also determined 8 h after vehicle or teduglutide injection (Figure 2F) at autopsy — i.e. ex vivo. In the teduglutide-injected non-ICR mice, intestine/HBS-ratio after 8 h was significantly increased compared to vehicle-injected non-ICR mice, suggesting intact recirculation (Figure 2G). In ICR mice, such increased intestine/HBS-ratio was not detectable at autopsy, suggesting disturbed recirculation in the ICR mice. In teduglutide injected ICR mice, body weight loss and stool water content increase on day 7 was numerically less pronounced. Teduglutide treatment did not have an effect on chow intake (Supplemental Fig. 1).

3.2. Pharmacologic GLP-2-stimulation acutely promotes biliary SeHCAT-retention in non-ICR mice

In previous studies, acute effects on gall bladder motility have been described for GLP-2 but not been found of functional relevance [8]. Thus, to study the acute effect of teduglutide on hepatobiliary bile acid retention in vivo, SeHCAT-distribution was determined on the Crystalcam 1 h before, and 1 h after injection of vehicle or teduglutide in non-ICR mice (Figure 3A). In vehicle-injected non-ICR mice, no change of signal distribution was notable, as indicated by unchanged focus ratio. After teduglutide-treatment, a strong accumulation of the SeHCAT-signal in projection to the gallbladder was detected and quantified by a significantly increased focus ratio (Figure 3B,C). This observation may suggest that the previously described acute effect of gall bladder relaxation is associated with acute retention of bile acids in the hepatobililary system.

3.3. Pharmacologic GLP-2-stimulation shifts the bile acid metabolome

To further characterize the functional relevance of teduglutide-mediated slowing of the EHC after ICR, the composition of the
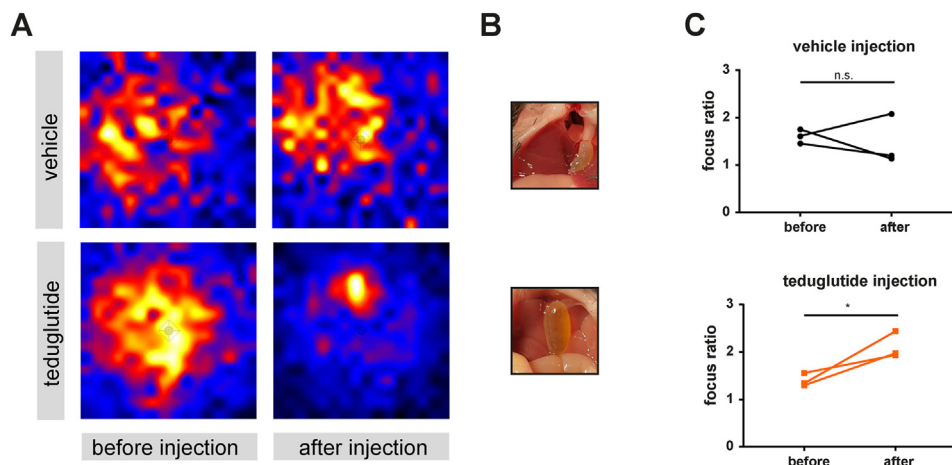
Figure 3: GLP-2 pharmacotherapy acutely promotes hepatobiliary retention. (A) Representative 2D-images from the CrystalCam before and after injection of vehicle or teduglutide treated mice in vivo. (B) Representative photographs of the gall bladder at autopsy. (F) In vivo focus ratio was calculated from images shown in (A) was calculated by normalizing to the area with the highest intensity, single data points, n = 3, mean, paired t-test.

plasma bile acid pool in sham, vehicle-injected ICR and teduglutide-treated ICR mice was analyzed. Plasma bile acid pool size was larger in both vehicle-injected ICR and teduglutide-treated ICR mice, compared to sham operated mice (1.55 ± 0.62 μmol/l vs. 1.50 ± 0.32 μmol/l vs. vs. 1.12 ± 0.34 μmol/l for veh ICR vs. ted ICR vs. sham). Plasma bile acid pool size was not increased by teduglutide

treatment. Compared to sham-operated mice, vehicle-injected ICR mice had a complete loss of secondary bile acids from their plasma. Primary bile acids were increased in vehicle-injected ICR mice compared to sham operated mice. In teduglutide-injected ICR mice, secondary bile acids were diminished as well (Figure 4A). However, in ICR mice, teduglutide induced a strong shift to conjugated bile acids
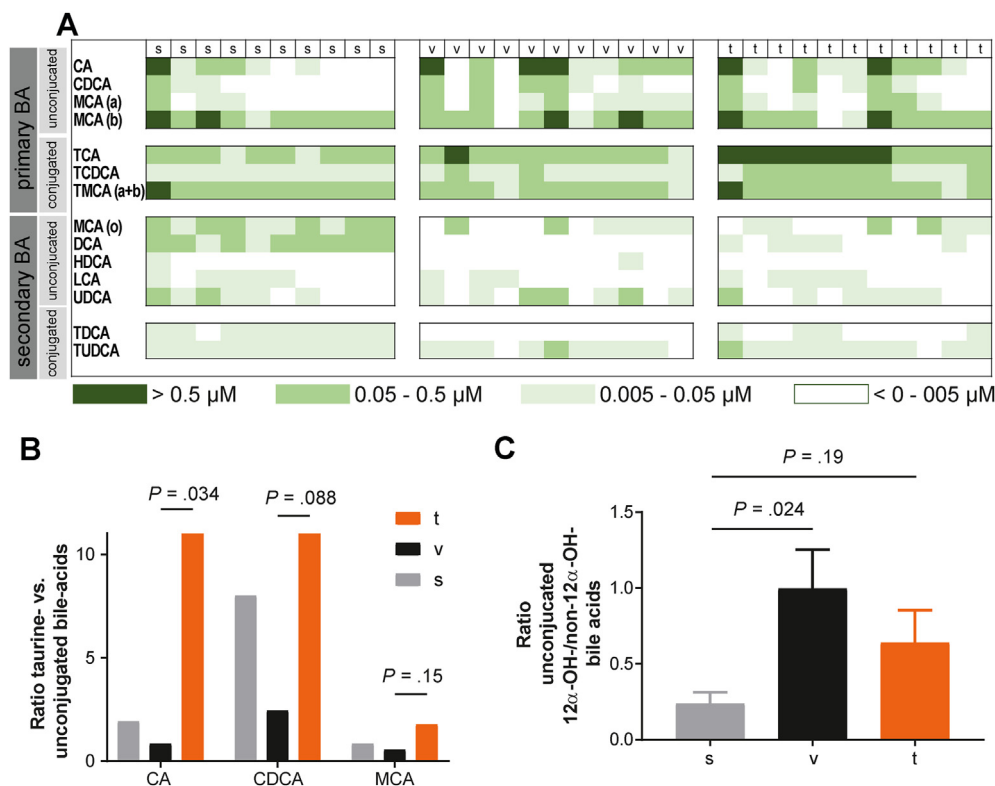
Figure 4: GLP-2 pharmacotherapy counteracts bile acid loss after ileocecal resection.
(A) heat-map of individual bile acids (rows) in individual mice (columns) s = sham operated; v = vehicle-injected ICR mice; t = teduglutide-injected ICR mice. (B) Ratio of taurine-conjugated vs. unconjucated bile acids was calculated for the 3 primary bile acid species, n = 10,11,11 (s, v, t), median, two-way-ANOVA, followed by Fisher's LSD-test. (C) Ratio of all measured unconjugated 12α-OH vs. non-12α-OH bile acids was calculated, n = 10,11,11 (s, v, t), mean ± SEM, One-way-ANOVA, followed by Dunn's test for multiple comparisons.

over unconjugated bile acids, as indicated by a significantly increased ratio of taurine-vs. unconjugated cholic acid (CA) (Figure 4B). Similar trends were observed for the other primary bile acids chenodeoxycholic acid (CDCA) as well as muricholic acids (MCA). Of note, the ratio of 12α-hydroxylated vs. non-12α-hydroxylated bile acids was significantly increased in vehicle ICR mice compared to sham operated mice. In contrast, the ratio of 12α−OH− to non-12α-OH bile acids was not significantly different in the teduglutide treated ICR mice compared to sham operated mice (Figure 4C). Of note, in non-ICR mice, GLP-2 pharmacotherapy induced a change of bile acid pool composition of both plasma and gall bladder bile towards the fasted state (Figure 5 A & B).

3.4. Pharmacologic GLP-2-stimulation promotes hepatic Fxr-dependent gene expression

Next, the bile acid signaling pathways in the ileum and the liver were analyzed on a transcriptional level. In the ileum, no significant changes of *Slc10a2* (Ileal sodium/bile acid cotransporter, IBAT) or *Fgf15* mRNA abundance by teduglutide were detected (Figure 6A,B). In the liver, *Fxr* expression was not significantly different after ICR and not changed by teduglutide. However, Shp (=*Nr0b2*) mRNA (nuclear receptor subfamily 0 group B member 2) expression was reduced after ICR, indicating reduced hepatic Fxr signaling. In the liver, consistent with severe bile acid loss, *Cyp7a1* was significantly induced in the ICR groups. Of note, teduglutide treatment did not significantly attenuate

this resection-triggered *Cyp7a1*-induction (Figure 7B). However, the *Cyp8b1* mRNA abundance was significantly reduced by teduglutide in non-ICR mice (Figure 7A). After ICR, significant *Cyp8b1*-reduction by teduglutide was also detectable when normalized to *Cyp7a1* (Figure 7C). In parallel to this specific *Cyp8b1* downregulation, we observed a significant upregulation of *Mafg* (MAF BZIP Transcription Factor G) by teduglutide both in healthy as well as in ICR mice. Taken together, the data are well in line with the notion that teduglutide promotes the beneficial non-12α-hydroxylated bile acid pool changes via MafG-associated Cyp8b1 reduction in ICR mice.

4. DISCUSSION

In the gut, GLP-2 pharmacotherapy promotes small intestinal villus growth by enhancing intestinal epithelial proliferation through stimulation of the GLP-2 receptor (GLP-2R), which is expressed in sub-epithelial myofibroblasts[19—22]. This effect can well be modeled in the ICR mouse model (Figure 1). The GLP-2 analogue teduglutide has a half-life of ~1 h in mice and thus repeated GLP-2-stimulation translates to a continuous and durable effect on small intestinal villus growth [23]. GLP-2 pharmacotherapy promotes intestinal absorption of water and electrolytes, in part by enhancing intestinal barrier function [24—27]. Following resection of the ileum, absorption capacity of the small bowel is reduced, but the reabsorption of bile acids is specifically reduced and results in disturbance of the EHC [28]. In the
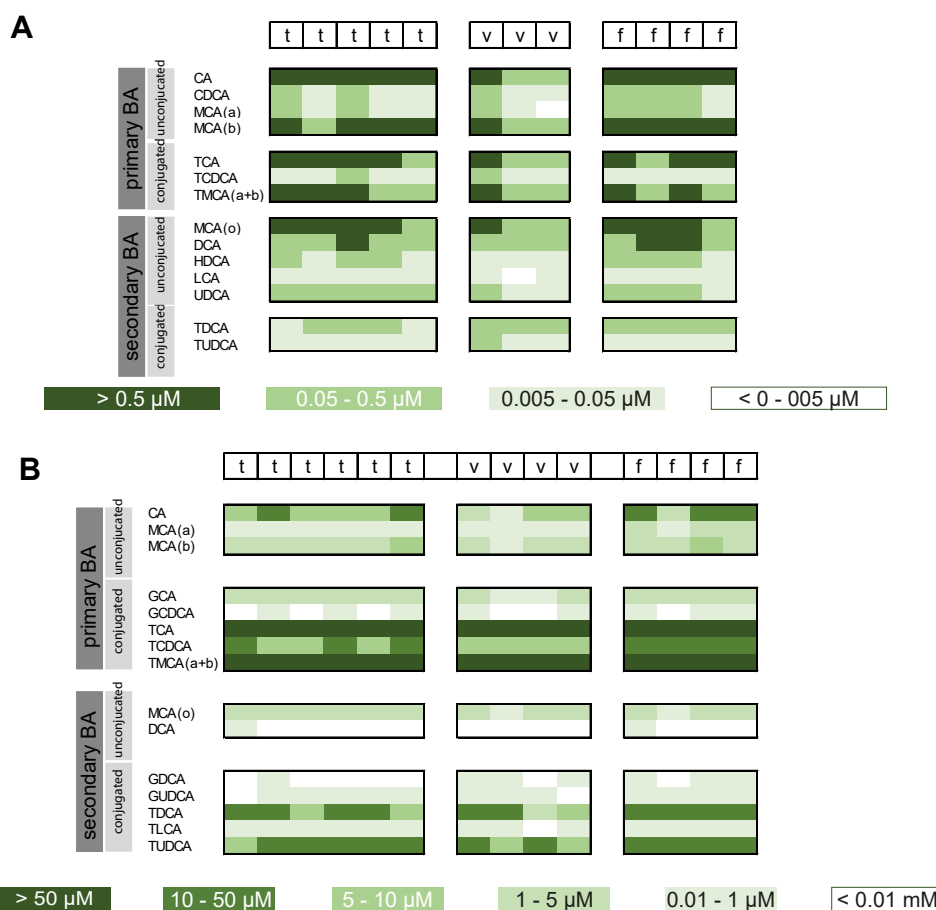
Figure 5: GLP-2 pharmacotherapy induces distinct plasma and bile acid pool changes in non-ICR mice. (A) Concentration heat-map of plasma individual bile acid species (rows) in individual mice (columns) t = teduglutide injected (n = 6) v = vehicle-injected (n = 4), f = fasted (n = 4). (B) Heat-map of biliary individual bile acid species (rows) in individual mice (columns) t = teduglutide injected v = vehicle-injected, f = fasted.
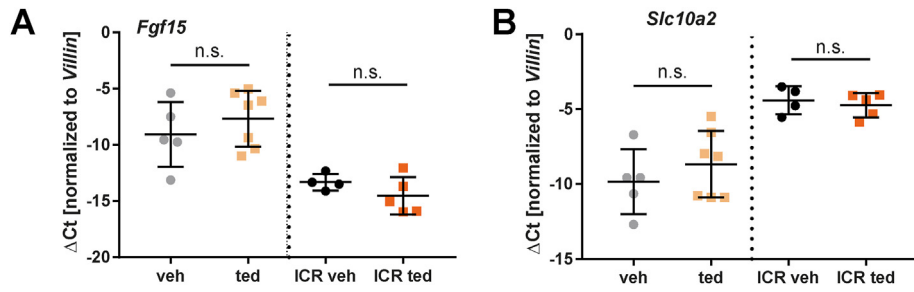
Figure 6: GLP-2 pharmacotherapy does not induce the major intestinal FXR-target genes. (A) In the small intestine, *Fgf15* mRNA expression was determined by qPCR and normalized to the epithelium specific marker *Villin*, n = 5,7,4,5 (vehicle-injected (veh), teduglutide-injected (ted), ICR veh, ICR ted), mean ± SD, unpaired t-test, decimal Y-axis. (B) In the small intestine, *Slc10a2* expression was normalized to *Villin*, n = 5,7,4,5 (veh, ted, ICR veh, ICR ted), mean ± SD, unpaired t-test, decimal Y-axis.
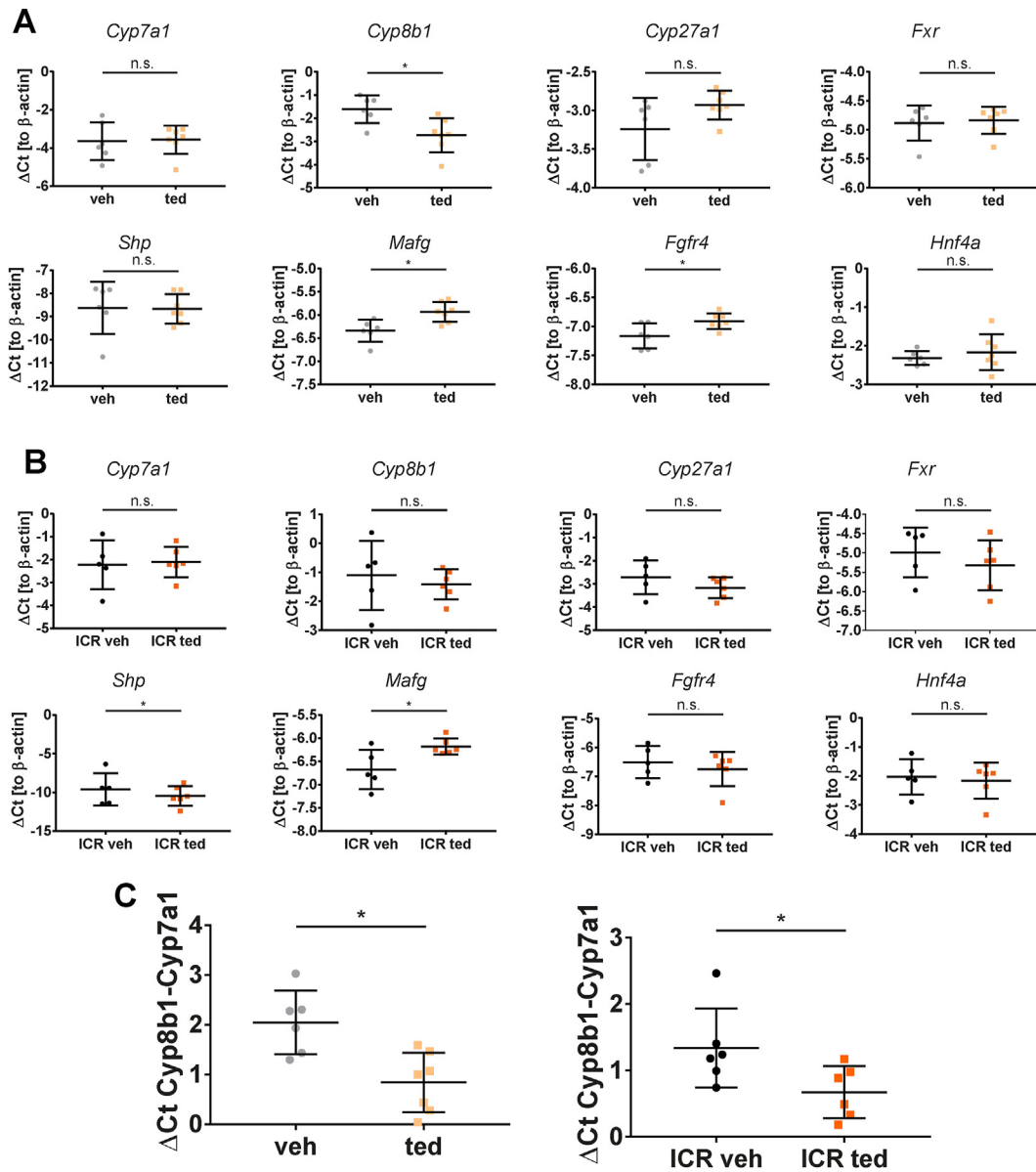
Figure 7: GLP-2 pharmacotherapy stimulates hepatic FXR-dependent signalling to reduce cyp8b1 expression. (A) In non-ICR mice, RNA expression was determined by qPCR in the liver, mean ± SD, unpaired t-test, decimal Y-axis. (B) In ICR mice, RNA expression was determined by qPCR in the liver, mean ± SD, unpaired t-test, decimal Y-axis. (C) Hepatic expression of Cyp8b1 was normalized to Cyp7a1, n = 6,7,6,6 (vehicle-injected (veh), teduglutide-injected (ted), ICR veh, ICR ted), mean ± SD, *p < 0.05, unpaired t-test, decimal Y-axis.

ICR mouse model, ~80% of ileum plus the cecum are resected, i.e., most of the site of active bile acid reabsorption, which at the same time reflects the primary site of *intestinal* Fxr-activity. Thus, after ICR, the accelerated EHC may be a potential druggable target of GLP-2 pharmacotherapy to counteract fecal bile acid losses and bile acid malabsorption.

It has previously been shown that in the gall bladder GLP-2 acts through the GLP-2R on subepithelial myofibroblasts to promote gall bladder relaxation [8]. The functional effect of GLP-2-dependent gall bladder relaxation on bile acid metabolism has previously been thought negligible, because hepatic bile flow, as measured by short-term catheterization of the common bile duct, was not altered by GLP-2-treatment in non-ICR mice [8]. Also, using knock-out mice, the presence of Glp2r expression has previously not been found essential for bile acid pool homeostasis in non-ICR mice [29]. However, it has been shown that GLP-2 pharmacotherapy affects bile acid metabolism, but the mechanisms have not been clarified [30—32].

Thus, we aimed to characterize the effect of teduglutide on enterohepatic circulation in mice by a novel, enhanced SeHCAT test (Figure 2A) using the portable 2D gamma camera,

First, SeHCAT retention was determined in ICR mice — modelling the most frequently encountered postoperative anatomy in humans receiving teduglutide. In these mice, SeHCAT retention was very low, confirming severe intestinal bile acid loss. Importantly, teduglutide significantly increased SeHCAT retention in ICR mice (Figure 2). Of note, SeHCAT elimination rate was significantly slowed by teduglutide compared to the vehicle injected ICR mice in the first 24 h but not thereafter, suggesting enhanced uptake of SeHCAT into the EHC by teduglutide. Of note, non-ICR teduglutide treated mice also had significantly increased SeHCAT retention compared to vehicle injected mice. This effect was somewhat unexpected, because mice with an intact ileum do not have bile acid loss which could be corrected by teduglutide. Thus, time-resolved spatial imaging was performed to study time-dependent changes of the distribution of the SeHCAT signal (Figure 3). Upon acute treatment with teduglutide (i.e. 1 h after injection), the SeHCAT signal was strongly accumulated in the hepatobiliary system, an effect which disappeared 12 h after injection. Importantly, at autopsy the teduglutide treated mice had prominently filled gall bladders as opposed to vehicle injected control mice, consistent with a relaxation effect by teduglutide.

Thus, in contrast to previous knowledge, our data suggest that the before described GLP-2 dependent acute relaxation of the gall bladder is indeed associated with acute retention of bile acids in the hepatobiliary system and slows enterohepatic circulation. Because this effect could be highly relevant after extensive ileocecal resection, we aimed to characterize the plasma bile acid pool along with signaling pathways in the intestine and the liver.

In the ileum, teduglutide did not induce significant changes in abundance of the prime FXR-target genes. While we cannot exclude that any GLP-2-dependent changes of FXR-dependent gene expression in the intestinal epithelium occur, this observation suggests that the *intestinal* pathway is far less involved in the GLP-2-effect on bile acid retention, as the ileocecum is the site of *intestinal* Fxr-activity and the major source of Fgf-15/19 (Figure 6).

After ICR, expression of the rate-limiting enzyme for de novo bile acid synthesis, i.e. *Cyp7a1*, was significantly induced in both resected groups in the liver (Figure 7), likely reflecting increased 7α-hydroxy-4-cholesten-3-one (7α-C4) synthesis[33—35]. However, teduglutide treatment did not attenuate this elevated *Cyp7a1*-induction. Instead, and much to our surprise, *Cyp8b1* mRNA abundance was significantly reduced by teduglutide under nonoperated conditions. A strong

reduction of *Cyp8b1* by teduglutide was also detectable in ICR mice. The 12-alpha-hydroxylase Cyp8b1 promotes the synthesis of cholic acid, a non-rate-limiting step in bile acid synthesis under steady state, when its substrate, 7α-C4, is present at regularly low concentrations. Cyp8b1 mediates the ratio of cholic acid to the non-12-alpha-hydroxylated bile acids chenodeoxycholic acid and muricholic acid.

Of note, after ICR and in the absence of teduglutide treatment, 12α-OH/non-12α-OH bile acid-ratio was significantly higher than in sham-operated mice. In contrast, in teduglutide treated ICR mice, this rise of 12α-OH/non-12α-OH bile acid-ratio was prevented.

Thus, our hypothesis is that after ICR, when 7α-C4 is compensatory generated through Cyp7a1 induction, indirect reduction of *Cyp8b1* by GLP-2-pharmacotherapy could result in 12-alpha-hydroxylation becoming the saturated and rate-limiting step for de-novo-generation of cholic acid to decrease the ratio of the primary unconjugated 12α-hydroxylated vs. non-12α-hydroxylated bile acids (Figure 8). While the *intestinal* Fxr-pathway is critical for suppressing both *Cyp7a1* and *Cyp8b1* gene expression, the *hepatic* Fxr-pathway, which is under control of the concentration of bile acids reaching the hepatocyte, is suppressing *Cyp7a1* to a far lesser extent than *Cyp8b1* [36], likely involving MafG signaling [11]. Consistently, and paralleled by this specific *Cyp8b1* downregulation, we observed an upregulation of *Mafg* by teduglutide both in healthy as well as in ICR mice. In ICR mice, this teduglutide stimulated *Mafg*-associated C*yp8b1* downregulation probably limits conversion of the increasingly synthetized 7α-C4 to the 12α-hydroxylated CA to favour conversion of 7α-C4 to non-12α-hydroxylated CDCA and MCA via Cyp27a1. Thus, our observations suggest that teduglutide influences the *hepatic* Fxr-pathway, which is activated by bile acids in the hepatocyte, by increasing recirculation of bile acids from the intestine, by increasing hepatobiliary retention, or, most likely, both (Figure 8). Increased hepatobiliary bile acid retention is likely mediated by the GLP-2R, expressed in myofibroblasts and hepatic stellate cells [37] This novel mechanism of GLP-2 action may in part be responsible for the unexpected failure to detect a dose-dependent downregulation of the severely increased fasting serum 7α-C4 concentrations by GLP-2-pharmacotherapy in jejunostomy patients [30], because in the setting of maximal bile acid synthesis, 7α-C4 levels may not reflect Cyp7a1 activity only, but also GLP-2-Fxr-MafG-reduced transformation via Cyp8b1.

Of note, loss of secondary bile acids after ICR was not prevented by teduglutide. However, teduglutide induced a striking shift to conjugated bile acids over unconjugated bile acids in ICR mice, as indicated by a significantly increased ratio of taurine-vs. unconjugated bile acids. While the 40% ICR mouse model is not a complete model of intestinal failure with short bowel syndrome (SBS) on parenteral nutrition, but rather a model of intestinal resection in mice, fully enterally fed, it is
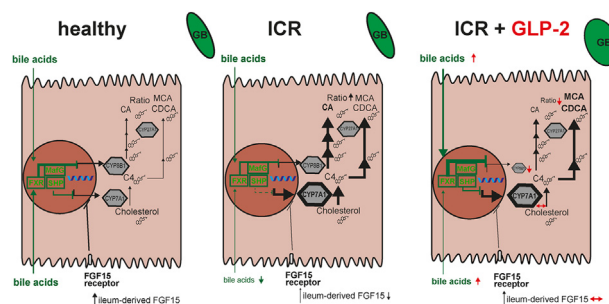
Figure 8: GLP-2 pharmacotherapy activates hepatic Fxr-signaling to attenuate resection-associated bile acid loss.

possible that the observations in bile salt pool changes do not completely translate to clinical scenarios. However, an increased prevalence of conjugated bile acids in the setting of SBS may be particularly aimed for because replacement therapy with conjugated bile acids has been shown to alleviate burden of urolithiasis by enhancing fat absorption and thus reducing calcium fatty acid soap formation and oxalate hyperabsorption [38], a frequently encountered complication of SBS [39]. Additionally, experiments in non-ICR mice showed that teduglutide induced specific changes in the bile acid pool composition of plasma and bile. GLP-2-pharmacotherapy seems to promote the interdigestive phase, ultimately optimizing conditions for the next digestive process (Figure 5).

Taken together, GLP-2-pharmacotherapy effects on bile acid recirculation and pool composition may be specifically important in the context of intestinal failure associated liver disease (IFALD): Genetic ablation of Cyp8b1, the enzyme increasing 12α-OH/non-12α-OH bile acid-ratio has been shown to preserve host metabolic function by repressing steatohepatitis and altering gut microbiota composition upon exposure to high carbohydrates [40]. If potentially beneficial GLP-2-pharmacotherapy effect on IFALD development is, as addressed with this ICR mouse model, more promising in patients with a colon in continuity, than with a jejunostomy, would require a well-controlled clinical trial. Nevertheless, normalization of the increased 12α-OH/non-12α-OH bile acid-ratio after ileocecal resection by teduglutide may be therapeutically considered potentially beneficial, because an increased 12α-OH/non-12α-OH bile acid-ratio is associated with insulin resistance [41,42] and lipogenesis [43]. It may thus be one hit which together with other factors (parenteral nutrition, systemic inflammation, increased intestinal permeability) may drive the development for IFALD [44], which puts the liver at risk to develop overt IFALD after another hit such as infection.

Therefore, we propose that pharmacologic GLP-2 treatment indirectly promotes *hepatic* Fxr signaling by increased bile acid recirculation from the intestine, as well as increased bile acid retention in the biliary system. Synergistically, these effects alleviate bile acid metabolome dysfunction and malabsorption resulting from loss of the ileocecum. The findings suggest that GLP-2 pharmacotherapy should be explored in diseases of relative or absolute impaired *hepatic* FXR signaling, such as IFALD, and also for other forms of bile acid malabsorption.

ACKNOWLEDGEMENTS

CRediT AUTHORSHIP CONTRIBUTION STATEMENT

Johannes Reiner: Writing — review & editing, Writing — original draft, Visualization, Validation, Methodology, Investigation, Funding acquisition, Formal analysis, Data curation, Conceptualization. **Nooshin Mohebali:** Writing — review & editing, Validation, Methodology, Investigation, Formal analysis, Data curation. **Jens Kurth:** Writing — review & editing, Supervision, Resources, Project administration, Methodology, Conceptualization. **Maria Witte:** Writing — review & editing, Supervision, Resources, Methodology, Conceptualization. **Cornelia Prehn:** Writing — review & editing, Visualization, Software, Methodology, Formal analysis. **Tobias Lindner:** Writing — review & editing, Methodology, Investigation, Formal analysis. **Peggy Berlin:** Writing — review & editing, Project administration, Methodology, Investigation, Formal analysis, Data curation. **Nagi Elleisy:** Writing — review & editing, Resources, Investigation. **Robert H. Förster:** Writing — review & editing, Formal analysis. **Alexander Cecil:** Writing — review & editing, Software. **Robert Jaster:** Writing — review & editing, Supervision, Resources, Project administration, Funding acquisition. **Jerzy Adamski:** Writing — review & editing, Visualization, Software, Methodology. **Sarah M. Schwarzenböck:** Writing — review & editing, Project administration, Methodology, Conceptualization. **Brigitte Vollmar:** Writing — review & editing, Supervision, Resources, Methodology. **Bernd J. Krause:** Writing — review & editing, Supervision, Resources, Methodology, Conceptualization. **Georg Lamprecht:** Writing — review & editing, Writing — original draft, Supervision, Resources, Methodology, Funding acquisition, Conceptualization.

DECLARATION OF COMPETING INTEREST

FUNDING SOURCES

DATA AVAILABILITY

Data will be made available on request.

APPENDIX A. SUPPLEMENTARY DATA

Supplementary data to this article can be found online at https://doi.org/10.1016/j.molmet.2025.102121.

REFERENCES

[1] Drucker DJ, Yusta B. Physiology and pharmacology of the enteroendocrine hormone glucagon-like peptide-2. Annu Rev Physiol 2014;76:561—83. https://doi.org/10.1146/annurev-physiol-021113-170317.

[2] Philippe J, Mojsov S, Drucker DJ, Habener JF. Proglucagon processing in a rat islet cell line resembles phenotype of intestine rather than pancreas. Endocrinology 1986;119(6):2833—9. https://doi.org/10.1210/endo-119-6-2833.

[3] Drucker DJ, Erlich P, Asa SL, Brubaker PL. Induction of intestinal epithelial proliferation by glucagon-like peptide 2. Proc Natl Acad Sci U S A 1996;93(15):7911—6. https://doi.org/10.1073/pnas.93.15.7911.

[4] Jeppesen PB, Pertkiewicz M, Messing B, Iyer K, Seidner DL, O'Keefe SJD, et al. Teduglutide reduces need for parenteral support among patients with short bowel syndrome with intestinal failure. Gastroenterology 2012;143(6):1473—1481.e3. https://doi.org/10.1053/j.gastro.2012.09.007.

[5] Jeppesen PB, Sanguinetti EL, Buchman A, Howard L, Scolapio JS, Ziegler TR, et al. Teduglutide (ALX-0600), a dipeptidyl peptidase IV resistant glucagon-like peptide 2 analogue, improves intestinal function in short bowel

syndrome patients. Gut 2005;54(9):1224—31. https://doi.org/10.1136/gut.2004.061440.

[6] Jeppesen PB, Gilroy R, Pertkiewicz M, Allard JP, Messing B, O'Keefe SJ. Randomised placebo-controlled trial of teduglutide in reducing parenteral nutrition and/or intravenous fluid requirements in patients with short bowel syndrome. Gut 2011;60(7):902—14. https://doi.org/10.1136/gut.2010.218271.

[7] Jeppesen PB, Gabe SM, Seidner DL, Lee H-M, Olivier C. Factors associated with response to teduglutide in patients with short-bowel syndrome and intestinal failure. Gastroenterology 2018;154(4):874—85. https://doi.org/10.1053/j.gastro.2017.11.023.

[8] Yusta B, Matthews D, Flock GB, Ussher JR, Lavoie B, Mawe GM, et al. Glucagon-like peptide-2 promotes gallbladder refilling via a TGR5-independent, GLP-2R-dependent pathway. Mol Metabol 2017;6(6):503—11. https://doi.org/10.1016/j.molmet.2017.03.006.

[9] Hansen NL, Brønden A, Nexøe-Larsen CC, Christensen AS, Sonne DP, Rehfeld JF, et al. Glucagon-like peptide 2 inhibits postprandial gallbladder emptying in man: a randomized, double-blinded, crossover study. Clin Transl Gastroenterol 2020;11(12):e00257. https://doi.org/10.14309/ctg.0000000000000257.

[10] Nguyen JT, Shaw RPH, Anakk S. Bile acids-A peek into their history and signaling. Endocrinology 2022;163(11). https://doi.org/10.1210/endocr/bqac155.

[11] Aguiar Vallim TQ de, Tarling EJ, Ahn H, Hagey LR, Romanoski CE, Lee RG, et al. MAFG is a transcriptional repressor of bile acid synthesis and metabolism. Cell Metab 2015;21(2):298—311. https://doi.org/10.1016/j.cmet.2015.01.007.

[12] Berlin P, Reiner J, Wobar J, Bannert K, Glass A, Walter M, et al. Villus growth, increased intestinal epithelial sodium selectivity, and hyperaldosteronism are mechanisms of adaptation in a murine model of short bowel syndrome. Dig Dis Sci 2019;64(5):1158—70. https://doi.org/10.1007/s10620-018-5420-x.

[13] Valdés Olmos RA, Taal BG, Hoefnagel CA, Boot H. Sequential 75SeHCAT imaging in addition to the conventional 75SeHCAT test: a necessity. Eur J Nucl Med 1995;22(2):181—2. https://doi.org/10.1007/BF00838950.

[14] Lewis MC, Brieaddy LE, Root C. Effects of 2164U90 on ileal bile acid absorption and serum cholesterol in rats and mice. JLR (J Lipid Res) 1995;36(5):1098—105. https://doi.org/10.1016/S0022-2275(20)39868-0.

[15] Sciarretta G, Vicini G, Fagioli G, Verri A, Ginevra A, Malaguti P. Use of 23-selena-25-homocholyltaurine to detect bile acid malabsorption in patients with ileal dysfunction or diarrhea. Gastroenterology 1986;91(1):1—9. https://doi.org/10.1016/0016-5085(86)90431-2.

[16] Pham HT, Arnhard K, Asad YJ, Deng L, Felder TK, St John-Williams L, et al. Inter-laboratory robustness of next-generation bile acid study in mice and humans: international ring trial involving 12 Laboratories. J Appl Lab Med 2016;1(2):129—42. https://doi.org/10.1373/jalm.2016.020537.

[17] McCreight LJ, Stage TB, Connelly P, Lonergan M, Nielsen F, Prehn C, et al. Pharmacokinetics of metformin in patients with gastrointestinal intolerance. Diabetes Obes Metabol 2018;20(7):1593—601. https://doi.org/10.1111/dom.13264.

[18] Scheurlen C, Kruis W, Büll U, Stellaard F, Lang P, Paumgartner G. Comparison of 75SeHCAT retention half-life and fecal content of individual bile acids in patients with chronic diarrheal disorders. Digestion 1986;35(2):102—8. https://doi.org/10.1159/000199353.

[19] Shin ED, Estall JL, Izzo A, Drucker DJ, Brubaker PL. Mucosal adaptation to enteral nutrients is dependent on the physiologic actions of glucagon-like peptide-2 in mice. Gastroenterology 2005;128(5):1340—53. https://doi.org/10.1053/j.gastro.2005.02.033.

[20] Dubé PE, Forse CL, Bahrami J, Brubaker PL. The essential role of insulin-like growth factor-1 in the intestinal tropic effects of glucagon-like peptide-2 in mice. Gastroenterology 2006;131(2):589—605. https://doi.org/10.1053/j.gastro.2006.05.055.

[21] Rowland KJ, Trivedi S, Lee D, Wan K, Kulkarni RN, Holzenberger M, et al. Loss of glucagon-like peptide-2-induced proliferation following intestinal epithelial insulin-like growth factor-1-receptor deletion. Gastroenterology 2011;141(6):2166—2175.e7. https://doi.org/10.1053/j.gastro.2011.09.014.

[22] Yusta B, Matthews D, Koehler JA, Pujadas G, Kaur KD, Drucker DJ. Localization of glucagon-like peptide-2 receptor expression in the mouse. Endocrinology 2019;160(8):1950—63. https://doi.org/10.1210/en.2019-00398.

[23] Reiner J, Berlin P, Wobar J, Schäffler H, Bannert K, Bastian M, et al. Teduglutide promotes epithelial tight junction pore function in murine short bowel syndrome to alleviate intestinal insufficiency. Dig Dis Sci 2020. https://doi.org/10.1007/s10620-020-06140-6.

[24] Benjamin MA, McKay DM, Yang PC, Cameron H, Perdue MH. Glucagon-like peptide-2 enhances intestinal epithelial barrier function of both transcellular and paracellular pathways in the mouse. Gut 2000;47(1):112—9. https://doi.org/10.1136/gut.47.1.112.

[25] Dong CX, Zhao W, Solomon C, Rowland KJ, Ackerley C, Robine S, et al. The intestinal epithelial insulin-like growth factor-1 receptor links glucagon-like peptide-2 action to gut barrier function. Endocrinology 2014;155(2):370—9. https://doi.org/10.1210/en.2013-1871.

[26] Reiner J, Berlin P, Held J, Thiery J, Skarbaliene J, Griffin J, et al. Dapiglutide, a novel dual GLP-1 and GLP-2 receptor agonist, attenuates intestinal insufficiency in a murine model of short bowel. JPEN J Parenter Enteral Nutr; 2021. https://doi.org/10.1002/jpen.2286.

[27] Reiner J, Thiery J, Held J, Berlin P, Skarbaliene J, Vollmar B, et al. The dual GLP-1 and GLP-2 receptor agonist dapiglutide promotes barrier function in murine short bowel. Ann N Y Acad Sci 2022;1514(1):132—41. https://doi.org/10.1111/nyas.14791.

[28] Boutte HJ, Chen J, Wylie TN, Wylie KM, Xie Y, Geisman M, et al. Fecal microbiome and bile acid metabolome in adult short bowel syndrome. Am J Physiol Gastrointest Liver Physiol 2022;322(1):G154—68. https://doi.org/10.1152/ajpgi.00091.2021.

[29] Patel A, Yusta B, Matthews D, Charron MJ, Seeley RJ, Drucker DJ. GLP-2 receptor signaling controls circulating bile acid levels but not glucose homeostasis in Gcgr-/- mice and is dispensable for the metabolic benefits ensuing after vertical sleeve gastrectomy. Mol Metabol 2018;16:45—54. https://doi.org/10.1016/j.molmet.2018.06.006.

[30] Hvistendahl MK, Naimi RM, Hansen SH, Rehfeld JF, Kissow H, Pedersen J, et al. Bile acid - farnesoid X receptor - fibroblast growth factor 19 axis in patients with short bowel syndrome: the randomized glepaglutide phase 2 trial. JPEN J Parenter Enteral Nutr; 2021. https://doi.org/10.1002/jpen.2224.

[31] Lim DW, Wales PW, Mi S, Yap JYK, Curtis JM, Mager DR, et al. Glucagon-like peptide-2 alters bile acid metabolism in parenteral nutrition—associated liver disease. JPEN - J Parenter Enter Nutr 2016;40(1):22—35. https://doi.org/10.1177/0148607115595596.

[32] Lim DW, Wales PW, Josephson JK, Nation PN, Wizzard PR, Sergi CM, et al. Glucagon-like peptide 2 improves cholestasis in parenteral nutrition—associated liver disease. JPEN - J Parenter Enter Nutr 2016;40(1):14—21. https://doi.org/10.1177/0148607114551968.

[33] Axelson M, Aly A, Sjövall J. Levels of 7 alpha-hydroxy-4-cholesten-3-one in plasma reflect rates of bile acid synthesis in man. FEBS Lett 1988;239(2):324—8. https://doi.org/10.1016/0014-5793(88)80944-x.

[34] Camilleri M, Nadeau A, Tremaine WJ, Lamsam J, Burton D, Odunsi S, et al. Measurement of serum 7alpha-hydroxy-4-cholesten-3-one (or 7alphaC4), a surrogate test for bile acid malabsorption in health, ileal disease and irritable bowel syndrome using liquid chromatography-tandem mass spectrometry. Neuro Gastroenterol Motil 2009;21(7):734-e43. https://doi.org/10.1111/j.1365-2982.2009.01288.x.

[35] Eusufzai S, Axelson M, Angelin B, Einarsson K. Serum 7 alpha-hydroxy-4-cholesten-3-one concentrations in the evaluation of bile acid malabsorption in patients with diarrhoea: correlation to SeHCAT test. Gut 1993;34(5):698—701. https://doi.org/10.1136/gut.34.5.698.

[36] Kong B, Wang L, Chiang JYL, Zhang Y, Klaassen CD, Guo GL. Mechanism of tissue-specific farnesoid X receptor in suppressing the expression of genes in bile-acid synthesis in mice. Hepatology 2012;56(3):1034—43. https://doi.org/10.1002/hep.25740.

[37] Fuchs S, Yusta B, Baggio LL, Varin EM, Matthews D, Drucker DJ. Loss of Glp2r signaling activates hepatic stellate cells and exacerbates diet-induced steatohepatitis in mice. JCI Insight 2020;5(8):e136907. https://doi.org/10.1172/jci.insight.136907.

[38] Emmett M, Guirl MJ, Santa Ana CA, Porter JL, Neimark S, Hofmann AF, et al. Conjugated bile acid replacement therapy reduces urinary oxalate excretion in short bowel syndrome. Am J Kidney Dis 2003;41(1):230—7. https://doi.org/10.1053/ajkd.2003.50012.

[39] Yang J, Sun H, Wan S, Mamtawla G, Gao X, Zhang L, et al. Risk factors for nephrolithiasis in adults with short bowel syndrome. Ann Nutr Metab 2019;75(1):47—54. https://doi.org/10.1159/000502329.

[40] Patankar JV, Wong CK, Morampudi V, Gibson WT, Vallance B, Ioannou GN, et al. Genetic ablation of Cyp8b1 preserves host metabolic function by repressing steatohepatitis and altering gut microbiota composition. Am J Physiol Endocrinol Metab 2018;314(5):E418—32. https://doi.org/10.1152/ajpendo.00172.2017.

[41] Uchida K, Makino S, Akiyoshi T. Altered bile acid metabolism in nonobese, spontaneously diabetic (NOD) mice. Diabetes 1985;34(1):79—83. https://doi.org/10.2337/diab.34.1.79.

[42] Haeusler RA, Astiarraga B, Camastra S, Accili D, Ferrannini E. Human insulin resistance is associated with increased plasma levels of 12α-hydroxylated bile acids. Diabetes 2013;62(12):4184—91. https://doi.org/10.2337/db13-0639.

[43] Lee J-Y, Shimizu H, Hagio M, Fukiya S, Watanabe M, Tanaka Y, et al. 12α-Hydroxylated bile acid induces hepatic steatosis with dysbiosis in rats. Biochim Biophys Acta Mol Cell Biol Lipids 2020;1865(12):158811. https://doi.org/10.1016/j.bbalip.2020.158811.

[44] Sasdelli AS, Agostini F, Pazzeschi C, Guidetti M, Lal S, Pironi L. Assessment of intestinal failure associated liver disease according to different diagnostic criteria. Clin Nutr 2019;38(3):1198—205. https://doi.org/10.1016/j.clnu.2018.04.019.